

Articles

Synthesis and Characterization of Long Chain Alkyl Acyl Carnitine Esters. Potentially Biodegradable Cationic Lipids for Use in Gene Delivery¹

Jinkang Wang, Xin Guo, Yuhong Xu, Lee Barron, and Francis C. Szoka, Jr.*

School of Pharmacy, University of California, San Francisco, California 94143-0446

Received March 25, 1998

A series of alkyl acyl carnitine esters (alkyl 3-acyloxy-4-trimethylammonium butyrate chloride) were synthesized as potential biocompatible cationic lipids for use in gene transfer. The physicochemical properties of the lipids, liposomes prepared from them, and their complexes with DNA were characterized by differential scanning calorimetry (DSC), particle size, ζ potential, and surface monolayer measurements. The transition temperatures and behavior at an air–water interface for this series are similar to phosphatidylcholines with the same hydrocarbon chain length. The physical properties of the L derivatives were not significantly different from the DL derivatives. At 70 °C, the acyl chains were readily hydrolyzed at pH 7. The influence of the aliphatic chain length ($n = 12–18$) on transfection efficiency in vitro was determined using cationic liposomes prepared from these lipids or their mixtures with the helper lipids, dioleoylphosphatidylethanolamine (DOPE), dioleoylphosphatidylcholine, monooleoylglycerol, and cholesterol (Chol). The mixture of myristyl 3-myristoyloxy-4-trimethylammonium butyrate chloride (MMCE, **4d**) with DOPE at a 1:1 molar ratio mediated the highest transfection efficiency in cell culture. The mixture of oleyl 3-oleoyloxy-4-trimethylammonium butyrate chloride (OOCE, **4f**) with Chol at a 1:1 molar ratio gave the highest transfection efficiency after intravenous administration in mice. In vivo gene expression using **4f** was comparable to values obtained with the best cationic lipids reported to date.

Introduction

Gene therapy has the potential to be an important therapeutic modality in the next century. This form of therapy treats disease by introducing exogenous sequences of DNA (genes) into cells to correct defective genes or to provide a new therapeutic gene product.² The challenge for the chemists is to create safe and effective nonviral systems for gene therapy. Positively charged polymers, peptides, and lipids have been studied as vehicles to transfer DNA across cell membranes.³ Of those molecules, cationic lipids have been the most extensively investigated,^{4–10} although the factors that control their effectiveness in vivo are still not understood. Our goal is to design a safe and efficient cationic lipid for gene delivery and report the synthesis and characterization of new cationic lipids based upon the naturally occurring carnitine. We also examined the influence of the aliphatic tail on transfection efficiency of the carnitine based lipids in vitro and in vivo.

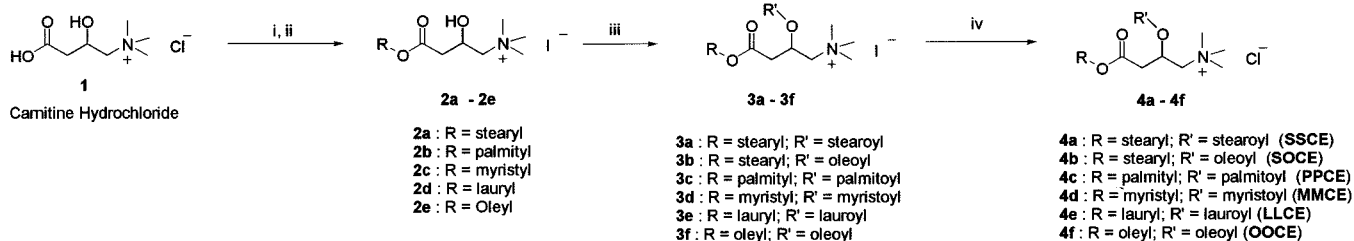
Carnitine **1** was detected at the beginning of this century, but it was not extensively studied until its importance in fatty acid metabolism was established 50 years later. Research on carnitine over the last 40 years focused on the effect of carnitine in metabolism and its role in fatty acid transfer into mitochondria.^{11–13} Its use as a gene delivery vehicle has not previously been investigated. Carnitine has a positively charged qua-

ternary amino group and β -hydroxy and γ -carboxylic acid groups. The latter two moieties can be coupled to hydrophobic chains. The structure of the resulting alkyl acyl carnitine ester is similar to the ester based cationic lipid DOTAP, but it contains one more methylene between the two linker groups, giving the region around the hydrophobic tails more conformational flexibility. The acyl group is an additional difference between the carnitine-based lipids and DOTAP. Although several approaches for the synthesis of short alkyl chain and medium or long acyl chain carnitine esters have been reported,^{14–19} the synthesis of long chain alkyl acyl carnitine ester is more difficult due to its limited solubility. We have developed a convenient route to prepare the long chain alkyl acyl carnitine esters **4a–f**. Liposomes prepared from these carnitine derivatives can efficiently complex with DNA and transfer the DNA complexes into cells in culture and in mice. The carnitine derivatives provide a biodegradable DNA delivery system for use in gene therapy.

Chemistry

Commercially available DL-carnitine monohydrochloride was used as the starting point for the synthesis. The synthesis of compounds **4a–f** is outlined in Scheme 1. DL-Carnitine monohydrochloride was treated with sodium hydroxide in ethanol to give the carnitine inner salt followed by alkylation with the appropriate alkyl iodide to yield the alkyl carnitine esters **2a–e**. Treatment of **2a–e** with the appropriate fatty acid anhydride

* Address correspondence to this author. Fax: (415) 476-0688. Telephone: (415) 476-3895. E-mail: szoka@cgl.ucsf.edu.

Scheme 1.^a Synthesis of Long Chain Alkyl Acyl Carnitine Esters

^a Reagents: (i) NaOH/C₂H₅OH; (ii) R-I/DMF-dioxane/120 °C; (iii) R'OR'/DMAP/CH₂Cl₂; (iv) anion-exchange chromatography.

in the presence of (dimethylamino)pyridine (DMAP) gave the alkyl acyl carnitine ester iodides **3a–f**. The easily oxidizable iodide was subjected to ion-exchange chromatography to yield the long chain DL-alkyl acyl carnitine ester chlorides **4a–f**. The L-alkyl acyl carnitine esters were prepared in a similar manner starting from L-carnitine.

Results and Discussion

Physicochemical Properties. The gel to liquid-crystal phase transition is a fundamental characteristic of bilayer membranes and indicates when the aliphatic chains undergo a transition from the all anti conformation to a mixed syn-anti conformation. When lipid systems are below their transition temperature the aliphatic chains are highly aligned. In the context of the formation of a cationic lipid DNA complex, it is difficult for the chains in the solid state to rearrange

and conform to DNA in the complex. Formation of a tightly packed DNA-lipid complex does not occur when the lipid is below its transition temperature. Moreover, the phase transition temperature (T_m) influences membrane fusion in model systems and might play a role during the introduction of the DNA into cells after the complex is internalized.⁸ Thus knowing the transition temperature of the lipids would help in predicting which of them were suitable candidates for gene transfer. Differential scanning calorimetry (DSC) was used to detect the T_m of the carnitine lipids. No pretransition peak was observed for the carnitine derivatives. Surprisingly, the transition temperature of the carnitine derivatives was very similar to the phosphatidylcholines of analogous chain length. The carnitine derivatives have a completely different interface between the aqueous and hydrocarbon region than the glycerol based lipids; they have an additional methylene group and

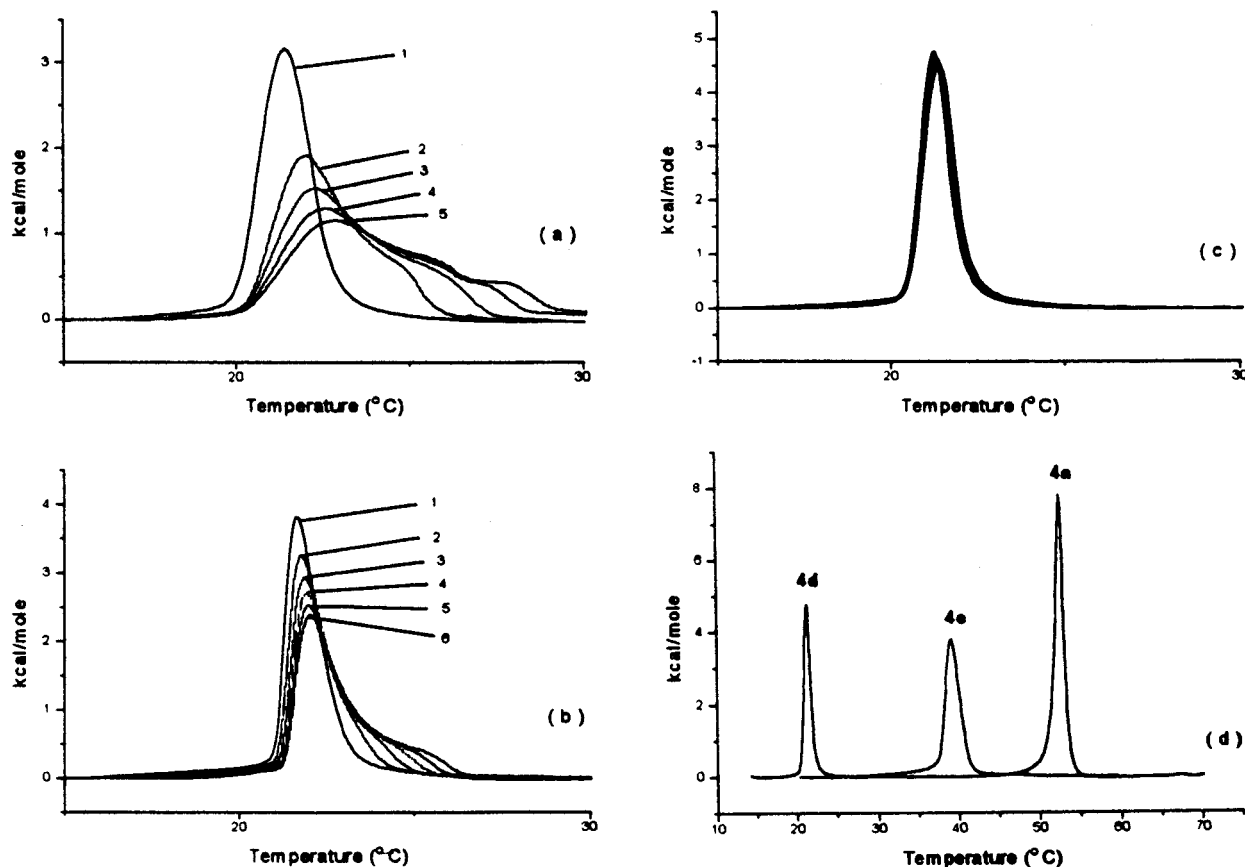


Figure 1. Differential scanning calorimetry of alkyl acyl carnitine ester chlorides. (a) Differential scanning calorimetry of **4d** (scanned from 10 to 70 °C), and the numbers stand for the scanning sequence. (b) Differential scanning calorimetry of **4d'** (scanned from 10 to 70 °C), and the numbers stand for the scanning sequence. (c) Differential scanning calorimetry of **4d** (scanned from 10 to 30 °C). (d) Comparison of the differential scanning calorimetry of alkyl acyl carnitine ester chlorides.

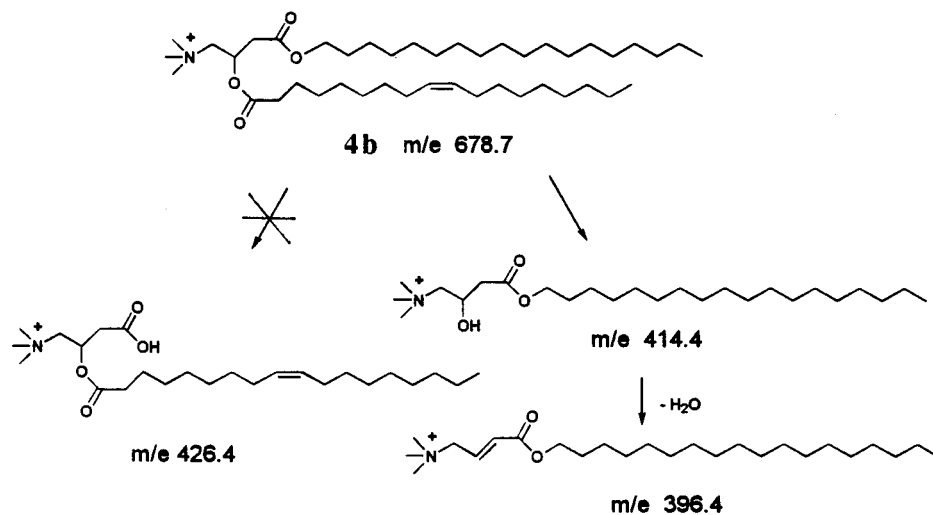


Figure 2. Potential hydrolysis products of alkyl acyl carnitine ester.

Table 1. Physical Properties of Alkyl Acyl Carnitine Ester Liposomes^a

lipids	ΔH (kcal/mol)	T_m (± 0.3 °C)	mean diameter ^b (nm)	range of particle diameter ^c (nm)	ζ potential ^g (mV)
4a	12.4 \pm 1	52.6	56	10–133	69.1
4a/DOPE ^d	ND ^f	ND ^f	83	10–750	60.8
4a/Chol ^e	ND ^f	ND ^f	88	10–316	38.9
4a'	11.7 \pm 1	53.3	ND ^f	ND ^f	ND ^f
4b	ND ^f	<10	81	37–133	48.0
4b/DOPE ^d	ND ^f	ND ^f	43	10–133	50.4
4b/Chol ^e	ND ^f	ND ^f	48	10–57	57.9
4c	8.7 \pm 0.8	39.2	70	10–205	56.8
4c/DOPE ^d	ND ^f	ND ^f	71	24–133	75.4
4c/Chol ^e	ND ^f	ND ^f	58	10–872	0.4
4d	5.5 \pm 0.5	21.3	84	10–205	46.4
4d/DOPE ^d	ND ^f	ND ^f	43	10–133	53.8
4d/Chol ^e	ND ^f	ND ^f	64	36–133	29.3
4d'	4.9 \pm 0.5	21.7	ND ^f	ND ^f	ND ^f
4e	ND ^f	<10	79	56–316	62.9
4e/DOPE ^d	ND ^f	ND ^f	73	56–133	88.9
4e/Chol ^e	ND ^f	ND ^f	73	56–873	4.4
4f	ND ^f	<10	74	10–87	34.3
4f/DOPE ^d	ND ^f	ND ^f	61	10–87	42.9
4f/Chol ^e	ND ^f	ND ^f	72	57–178	36.1

^a In water. ^b Obtained from the cumulant results of dynamic light scattering, with standard deviation (30–40%). ^c Obtained from the raw intensity results of dynamic light scattering. ^d Equimolar ratio. ^e 5:4 molar ratio. ^f ND = not determined. ^g With a standard deviation of 5–10 mV.

they lack a phosphate group; both factors would make the interfacial region more hydrophobic. Thus one might have expected a higher transition temperature. As in the case of phosphatidylcholine lipids, the phase transition temperature (T_m) of carnitine-based lipids increased with increasing hydrophobic chain length (Figure 1d). The chirality of the carnitine had no significant effect on the transition temperature of the lipids (compare the T_m for **4a/4a'** and **4d/4d'**, Table 1). The addition of an unsaturated acyl chain substantially decreased the transition temperature, which was too low (<10 °C) to be detected by the calorimeter used in these studies. The results of the DSC measurements are summarized in Table 1. Due to the appearance of shoulders in the thermogram upon repetitive scanning, the data for **4a** and **4c** are from the initial scan.

Repetitive DSC scanning from 10 to 70 °C resulted in the appearance of high-temperature shoulder peaks

either in water or HEPES buffer (pH 7.4). These peaks became bigger as the number of scans increased (Figure 1a,b). When the scanning was restricted to the lower temperatures (10–30 °C), no such shoulders or new peaks were observed (Figure 1c).

The shoulders on the thermogram resulted from a partial hydrolysis of the alkyl acyl carnitine ester. On the basis of a TLC and mass analysis of the lipid mixture after heating, hydrolysis occurred predominantly at the acyl chain rather than the alkyl chain. After DSC measurements the liposome suspensions were extracted with chloroform and the chloroform solution was dried over sodium sulfate. The TLC analysis of the chloroform solution showed two additional spots, neither of which was a long chain alkyl alcohol. The mass analysis of the chloroform solution of compound **4b** showed two peaks at *m/e* 414.4 and *m/e* 396.4 that indicated the presence of the acyl chain cleavage product and its elimination product. No peak at *m/e* 426.4 was found to support the cleavage of alkyl chain (Figure 2). It has been reported that the rate of hydrolysis of longer acyl chain carnitine esters is faster than shorter acyl chains.²⁰ These studies were performed under strongly basic conditions.^{20,21} In the cationic liposome, the hydrolysis of alkyl acyl carnitine esters occurs at pH 7.0 or 7.4 at relatively high temperatures. This may be due to a higher interfacial pH at the liposome bilayer because of the Cl⁻-OH⁻ anion exchange (Figure 3). The hydroxide at the reaction center could then accelerate the hydrolysis of the carnitine lipids. The reason for the selected cleavage of the acyl chain over the alkyl chain is not clear, but may be related to the orientation of the ester bond at the interface.

Compounds **4b**, **4c**, **4d**, **4d'**, and **4f** were selected for the monolayer studies since their transition temperatures were similar to the extensively studied diacyl phospholipids.²² Moreover, a number of the more active cationic lipids reported to date^{4,6,8} have fluid chains at 37 °C. Thus in any attempt to understand the complete mechanism of action of the cationic lipids one will have to account for the surface properties of these lipids. The data are summarized in Table 2. The compound **4d** had the same monolayer properties as **4d'** (Figure 4 and Table 2). This indicated that the chirality of the lipids

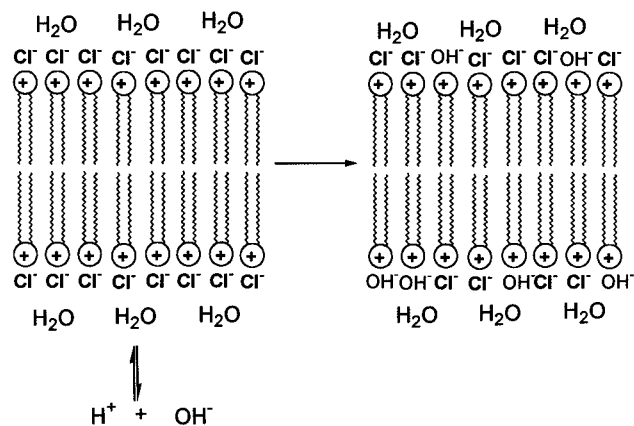


Figure 3. Schematic representation of the pH change at interface of water and lipid bilayer.

Table 2. Monolayer Parameters of Carnitine Derivatives^a

	4b	4c	4d	4d'	4f
mean molecular area A (\AA^2) (± 5)	70	66	74	72	82
collapse molecular area A_c (\AA^2) (± 2)	43	44	38	37	50
collapse surface pressure π_c (mN/m) (± 2)	46	52	51	50	46
collapse surface potential ΔV_c (mV) (± 30)	660	850	740	780	600

^a Measured in pH 7.4 HEPES buffer with 0.15 M NaCl.

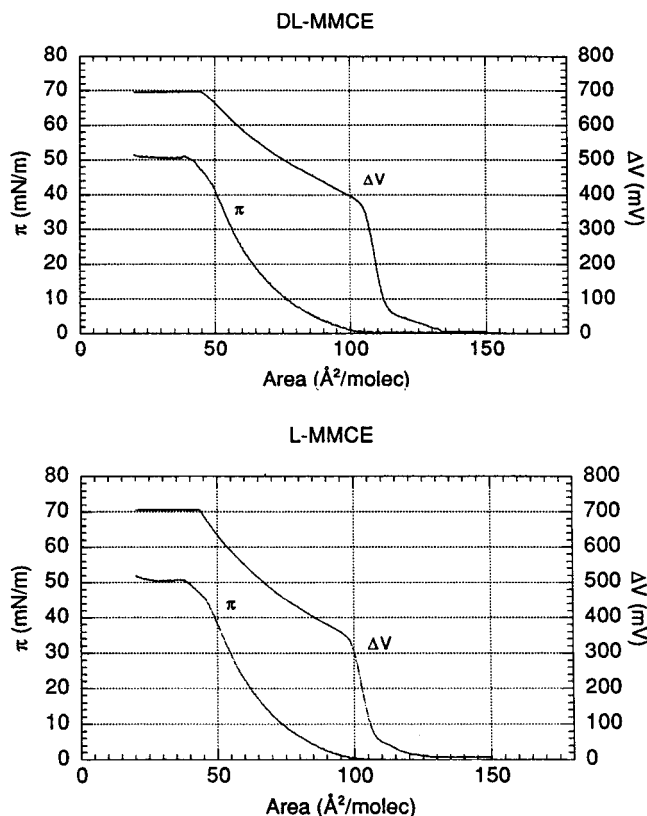


Figure 4. Monolayer study of **4d** (DL-MMCE) and **4d'** (L-MMCE).

had little influence on the packing of the lipids in the monolayer. The difference in the collapse molecular area of **4c** and **4d** indicated that the longer hydrophobic chain occupied more space than the shorter chain. Lipid **4c** has a lower charge density than **4d** but had a higher collapse surface potential than **4d**. This is a result of the larger vertical component of the dipole moments (μ_{\perp})

of the lipid.²³ Lipid **4f** with a cis double bond in both hydrophobic chains has the largest mean and collapse molecular areas and the lowest collapse surface potential, consistent with a more expanded monolayer. As shown below, the most active lipid for in vivo transfection is **4f**, which has the most expanded bilayer and the lowest collapse surface potential whereas other lipids such as **4c** or **4d** which have a higher surface charge density are less active. One interpretation for these data is that there is a delicate balance between the factors required for assembly of the complex to provide a suitable delivery vehicle and disassembly of the complex when it arrives at its target site so that the DNA can be transcribed.

The data from the monolayer studies are consistent with measurements of the ζ potential of the liposomes prepared from the various lipids. Carnitine derivatives that had the highest charge density as evaluated by collapse surface potential divided by mean molecular area (Table 2) had the highest ζ potential (Table 1). The ζ potential and particle size play an important role in the interaction of lipid vesicles with biological membranes^{3b,8,24,25} and may effect the gene transfection mechanism and efficiency. This is because the cell surface carries a net negative charge and the positively charged cationic lipid–DNA complexes interact with the cell surface via electrostatic interactions.

The carnitine derivatives can form liposomes either alone or in the presence of helper lipids such as DOPE and Chol. Liposomes formed by a sonication method had diameters that range from 40 to 90 nm (Table 1). The diameters are not greatly effected by addition of DOPE or Chol. In the presence of DNA, the diameter of the complexes increases as the charge ratio approaches 1:1 (Table 3). This increase in diameter is caused by a membrane alteration when the positively charged lipids interact with the negative charges on the DNA.²⁶ If the lipids are in their fluid state, i.e., above the transition temperature, they can rearrange. The complexes can also aggregate and form large particles over time. This aggregation is characteristic of polyelectrolyte complexes that are formed close to charge neutrality and is one of the reasons that more effective gene transfer from the cationic lipids is observed at positive charge ratios of about 2/1 or greater.

Liposomes prepared from carnitine derivatives with and without the helper lipids showed positive ζ potential values from 30 to 90 mV (Table 1). The ζ potential of the lipid–DNA complexes decreases as the charge ratio approaches 1 (Table 3). The physicochemical data, in conjunction with the biological studies reported below, show that effective cationic carnitine derivatives have fluid aliphatic chains at 37 °C and that the more active derivative in both the in vitro (**4d**) and in vivo (**4f**) situation is the derivative that has a lower charge density. In the future, computational approaches for modeling of cationic lipid–DNA complexes will be feasible and the physicochemical data on the carnitine derivatives will be a valuable data set to validate results from such computation.

Biological Results and Discussion

The cationic carnitine derivatives **4a–f** were tested for their ability to deliver a plasmid encoding a β -galactosidase gene as well as for their cytotoxicity in CV-1

Table 3. ζ Potential^a and Particle Size of Carnitine Derivative–DNA Complexes^b

lipid composition	charge ratio ^c (\pm , 1:1)			charge ratio ^c (\pm , 2:1)			charge ratio ^c (\pm , 4:1)		
	ζ potential (mV)	mean diameter ^d (nm)	range of particle diameter ^e (nm)	ζ potential (mV)	mean diameter ^d (nm)	range of particle diameter ^e (nm)	ζ potential (mV)	mean diameter ^d (nm)	range of particle diameter ^e (nm)
4a	ND ⁱ	357	133–1150	ND ⁱ	74	56–316	ND ⁱ	ND ⁱ	ND ⁱ
4a/DOPE^f	-43.5	456	87–750	14.4	100	56–487	13.6	127	56–205
4a/Chol^g	-42.1	161	133–316	12.1	168	87–316	13.0	102	87–133
4b	ND ⁱ	754	205–1150	ND ⁱ	243	133–487	ND ⁱ	ND ⁱ	ND ⁱ
4b/DOPE^f	6.3	361	87–750	15.5	175	56–487	17.5	82	56–133
4b/Chol^g	7.2	358	316–487	11.8	125	100–178	14.0	100	56–205
4c	ND ⁱ	18050 ^h	1780–20000	ND ⁱ	174	56–487	ND ⁱ	ND ⁱ	ND ⁱ
4c/DOPE^f	8.9	342	133–1780	13.6	150	86–487	14.5	90	57–133
4c/Chol^g	-14.0	294	205–487	13.3	125	87–205	12.6	97	87–133
4d	ND ⁱ	5650 ^h	1150–10000	ND ⁱ	306	133–1780	ND ⁱ	ND ⁱ	ND ⁱ
4d/DOPE^f	-43.9	342	87–1150	14.9	168	56–487	13.3	89	56–133
4d/Chol^g	-42.9	253	133–487	12.5	151	87–316	13.9	114	87–205
4e	ND ⁱ	13300 ^h	1780–20000	ND ⁱ	175	133–1780	ND ⁱ	ND ⁱ	ND ⁱ
4e/DOPE^f	-40.5	386	133–750	13.6	175	87–750	12.3	94	86–133
4e/Chol^g	-45.1	330	205–750	14.9	150	87–316	11.7	105	56–205
4f	-7.2	1600	1150–1780	4.47	124	87–205	19.6	73	10–87
4f/DOPE^f	13.7	143	87–205	16.7	92	56–487	21.1	78	10–133
4f/Chol^g	5.6	205	100–562	9.5	116	87–205	10.2	87	56–133

^a Each measurement has a standard deviation of 5–10 mV. ^b The complexes were made at room temperature in water. ^c Ratio of quarternary nitrogen of carnitine derivatives/phosphate of DNA. ^d Obtained from cumulant results of dynamic light scattering, with standard deviation (30–40%). ^e Obtained from the raw intensity results of dynamic light scattering. ^f Equimolar ratio. ^g 5:4 molar ratio. ^h The standard deviations were very broad. ⁱ ND = not determined.

Table 4. Comparison of the Effects of the Cationic Carnitine Derivatives on β -Galactosidase Expression (in milliunits) in CV-1 Cell Culture^a

lipid composition	charge ratio (\pm)			
	1:1	2:1	4:1	8:1
4a	0.057	0.070	0.081	0.090
4a/DOPE^b	0.083	0.132	0.101	0.082
4a/Chol^c	0	0	0	0
4b	0.077	0.099	0.093	0.089
4b/DOPE^b	0.099	0.127	0.190	0.086
4b/Chol^c	0	0.046	1.058	0.133
4c	0.074	0.090	0.101	0.106
4c/DOPE^b	0.152	0.289	0.438	0.148
4c/Chol^c	0	0	0.454	0
4d	0.083	0.083	0.136	0.166
4d'	0.077	0.078	0.089	0.092
4d/DOPE^b	3.805	1.422	1.071	0.086
4d/Chol^c	0	0.033	2.011	0.480
4d/MOG^b	0.977	0.001	0.108	0.555
4d/DOPC^b	0.102	0.101	0.115	0.119
4e	0.001	0	0	0
4e/DOPE^b	0.354	1.001	2.120	0.268
4e/Chol^c	0.126	0	0.058	0.153
4f	0	0.039	0.431	0.196
4f/DOPE^b	0	0.112	0.217	0
4f/Chol^c	0.063	0.585	0.720	0.351
DOTAP	0.094	0.294	0.840	0.291

^a Cationic lipids were complexed with 600 ng/well of β -gal plasmid DNA to produce charge ratios (\pm) ranging from 1:1 to 8:1. The reported values are the mean of 21 transfection assays, with a coefficient of variation of \pm 20%. ^b Equimolar ratio. ^c 5:4 molar ratio.

cell culture. In Table 4 we compare the effect of cationic lipids **4a–f** on the transfection efficiency in vitro. The cationic carnitine derivatives **4a–f** alone demonstrated poor transfection efficiency at any charge ratio when compared with the widely used DOTAP. However, certain liposome formulations with helper lipids (**4d/DOPE**, **4d/Chol**, and **4e/DOPE**) mediated significantly more efficient expression of β -galactosidase reporter gene compared with DOTAP at their optimal charge ratio. The optimal charge ratio for the highest transfection efficiency of the carnitine derivative/DOPE mixtures depended upon the acyl chain. The enanti-

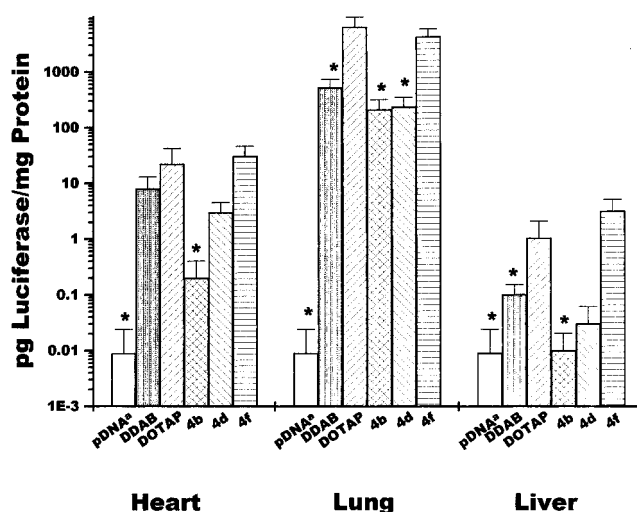


Figure 5. Luciferase reporter gene expression after intravenous injection of DNA–carnitine lipid complexes. Cholesterol was included as the helper lipid in all treatments at an equimolar ratio relative to cationic lipid. The charge ratio (\pm) for all DNA–carnitine lipid complexes was 5:1. ^aPlasmid DNA. *Paired *t*-test significant difference at $P \leq 0.05$ vs DOTAP/Chol.

omer **4d'** and racemic mixture **4d** had the same optimal charge ratio, and **4d'** mediated similar levels of transfection as **4d**. In the presence of DOPE, a 14-carbon hydrophobic chain (**4d**, MMCE) afforded the most efficient transfection, and the in vitro transfection activity of the alkyl acyl carnitine esters follows the order of **4d** > **4e** > **4b** > **4f** > **4c** > **4a**.

On the basis of the in vitro transfection results as well as reports in the literature,²⁷ we evaluated the activity of **4b**, **4d**, and **4f** to deliver a plasmid encoding luciferase into the heart, lung, and liver of female ICR mice after intravenous administration (Figure 5). The activity of the carnitine derivatives was compared to two cationic lipids widely used for in vivo gene transfer, DOTAP²⁷ and DDAB.²⁷ In the specified formulation (charge ratio

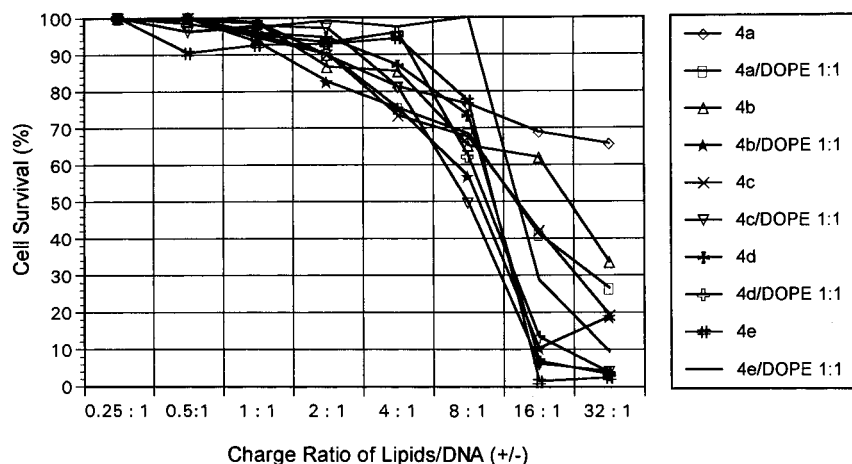


Figure 6. Comparison of the cytotoxicity of DNA–carnitine derivative complexes in CV-1 cell culture. Cationic carnitine lipids at a range of concentrations were complexed with 600 ng/well of β -gal plasmid DNA to produce charge ratio (\pm) ranging from 0.25:1 to 32:1. The survival percentage of treated cells was tested and compared with untreated cells.

+/- = 5:1, with equimolar Chol as the helper lipid) **4f** provided the best transfection activity. Smyth-Templeton and co-workers²⁷ have reported that DOTAP/Chol is the most effective cationic lipid mixture for mediating gene transfer in the lung after intravenous administration. In all three tissues, the mixture of **4f** with Chol mediated better luciferase expression than DDAB and mediated as efficient luciferase expression as the mixture of DOTAP/Chol.²⁷

Although cationic lipids are widely used in cell biology, there have been few attempts to explore the relationship between chemical structure and transfection activity.^{9,28} This is partially due to the multistep nature of the process which involves the following. The cationic liposomes interact with anionic DNA by electrostatic forces, which results in a change in the membrane properties of the liposome and a compaction of the DNA.²⁸ The DNA–liposome complexes must then adhere to the cell membrane.^{6,29,30} Although the mechanism of entry into the cell is not fully understood, a number of studies indicate that the complex is endocytosed.^{4,8,29} The DNA must then escape from the endosome, dissociate from the cationic lipid, and enter the nucleus for the gene to be expressed.³⁰

Akao and co-workers synthesized a series of double-chain ammonium amphiphiles and correlated the transfection efficiency with the physicochemical properties.²⁸ They concluded the vesicles in the fluid state were considerably more efficient than the vesicles in the solid state. Our data with the carnitine lipids support this suggestion. Two other groups have compared transfection activity and toxicities of various cationic lipids but did not examine the physical properties of the resulting liposomes. The Felgner group investigated a series of monovalent cationic headgroups with two hydrocarbon chains attached to the headgroup by either ester or ether linkages.⁹ The rank order of transfection activity of their lipids was C14:0 > C18:1 > C16:0 > C18:0, which is similar to what we observe with the carnitine derivatives. Although they did not measure the transition temperature of the derivatives, it is likely that they have a similar transition temperature–chain length relationship as the alkyl acyl carnitine lipids. Therefore, in transfection experiments, the more active lipids both in vitro and in vivo are in the fluid state at 37 °C.

The extensive physical characterization of the carnitine lipids and the resulting liposomes formed from these lipids indicate that the fluid bilayers composed of **4d** are more active than **4b**, **4e**, or **4f** in CV-1 cells. The ζ potential of the complexes must be positive to observe good activity. However, as others have noted,²⁷ the correlation between in vitro and in vivo activity is not particularly strong. All of the derivatives that are active in vitro show activity in vivo, but the best in vivo transfection efficiency is obtained with **4f**. This lipid has the most expanded headgroup area and the highest fluidity in the aliphatic chains. This may provide a better packing of the aliphatic chains in the complex with DNA, while also allowing such packing interactions to be readily reversed by biomolecules in the tissue to release the DNA after intravenous injection.³⁰

Cytotoxicity of cationic lipids **4a–e** alone or in composition with DOPE was tested by MTT reduction method.³¹ Figure 6 shows the comparison of the cytotoxicity of DNA–carnitine derivative complexes in CV-1 cell culture. The cell survival was >75% at charge ratio 4:1 and >80% at 2:1. Thus all of cationic carnitine derivatives **4a–e** were well tolerated at the optimal charge ratio for transfection. In the cases of **4a–d**, the addition of DOPE somewhat decreased the cell survival. Currently the in vivo toxicity of **4f** is being evaluated to learn if the carnitine template can overcome some of the toxic manifestations observed from other cationic liposomes in vivo.

Conclusions

We have designed and developed a convenient synthetic route to prepare cationic alkyl acyl carnitine esters that are potentially biocompatible lipids for gene delivery. The optimal length of the hydrophobic chains are 14 carbons for in vitro transfection. Very high in vivo transfection is obtained after intravenous administration of complexes formed from the mixture of the alkyl acyl carnitine ester **4f** containing C18:1 aliphatic chains and cholesterol.

Experimental Section

General Procedures and Materials. ¹H NMR (300 MHz) spectra were recorded in CDCl₃ with Me₄Si as internal standard. *J* values are in hertz. Liquid secondary ion mass spectra were obtained at the Mass Spectrometry Facility,

University of California at San Francisco. TLC analyses of lipids were performed on 0.25-mm silica gel plates. DMF was distilled from CaH_2 , CH_2Cl_2 was distilled from P_2O_5 , and THF was distilled from Na metal and benzophenone. Column chromatography was performed with silica gel (Aldrich, 230–400 mesh). Unless noted otherwise, the ratios describing the compositions of solvent mixtures represent relative volumes. Elemental analyses were performed by Microanalytical Lab, University of California at Berkeley. The lipids DOPE and DOTAP were purchased from Avanti Polar Lipids, Alabaster, AL. All other organic chemicals were purchased from Aldrich. CV-1 cells (monkey fibroblast) were provided by the UCSF cell culture facility. Female ICR mice were obtained from Simonsen (Gilroy, CA). All animals were handled in accordance with protocols described by the National Institutes of Health Guidelines for the Care and Use of Laboratory Animals, and with the approval of the Committee of Animal Research at the University of California, San Francisco. Animals were sacrificed at the stated times with a sodium pentobarbital overdose. Plasmids pCMV- β Gal and RSV-Luc were grown in *Escherichia coli*, then extracted, and purified by two centrifugations in equilibrium on CsCl gradients. The plasmid DNAs were subjected to two CsCl gradients to ensure purity and had less than 20 endotoxin units per milligram of DNA as measured by the Whitaker Biotechnology endotoxin detection kit.

General Procedure for the Preparation of Alkyl Carnitine Esters. Examples: Stearyl Carnitine Ester (2a). A solution of DL-carnitine hydrochloride (1.0 g, 5.05 mmol) and sodium hydroxide (0.303 g, 7.58 mmol) in ethanol (15 mL) was stirred at room temperature for 2 h. The resulting white precipitate (NaCl) was removed by filtration, and the solvent was evaporated under reduced pressure to give a white solid, carnitine inner salt. A suspension of the carnitine inner salt and 1-iodooctadecane (2.31 g, 6.06 mmol) in DMF–dioxane (3:5, 40 mL) was heated with an oil bath at 120 °C under argon for 4 h. The solvent was removed by a rotary evaporator followed by high vacuum, and the residue was resolved by chromatography on a silica gel column using $\text{CH}_3\text{OH}-\text{CHCl}_3$ as eluant to give 2.22 g (81%) of stearyl carnitine ester (2a) as a white solid: $^1\text{H NMR}$ (CDCl_3) δ 4.79 (m, 1 H), 4.43 (d, $J = 5.3$, 1 H), 4.09 (t, $J = 6.9$, 2 H), 4.03 (d, $J = 13.0$, 1 H), 3.67 (dd, $J = 10.3$, 13.3, 1 H), 3.51 (s, 9 H), 2.79 (dd, $J = 5.7$, 17.0, 1 H), 2.66 (dd, $J = 7.0$, 17.1, 1 H), 1.80–1.60 (m, 4 H), 1.26 (brd s, 28 H), 0.88 (t, $J = 6.6$, 3 H); LSIMS (NBA) m/e 414.4 for $\text{C}_{25}\text{H}_{52}\text{NO}_3$ (cation).

By this procedure were prepared the following alkyl carnitine esters.

Palmityl carnitine ester (2b): yield 65%; $^1\text{H NMR}$ (CDCl_3) δ 4.78 (m, 1 H), 4.44 (d, $J = 5.4$, 1 H), 4.09 (t, $J = 6.9$, 2 H), 3.65 (dd, $J = 10.2$, 13.3, 1 H), 3.58 (d, $J = 5.1$, 1 H), 3.51 (brd s, 9 H), 2.80 (dd, $J = 5.7$, 17.2, 1 H), 2.66 (dd, $J = 7.1$, 17.1, 1 H), 1.65 (broad m, 4 H), 1.26 (brd s, 24 H), 0.88 (t, $J = 0.66$, 3 H); LSIMS (NBA) m/e 386.2 for $\text{C}_{23}\text{H}_{48}\text{NO}_3$ (cation).

Myristyl carnitine ester (2c): yield 74%; $^1\text{H NMR}$ (CDCl_3) δ 4.79 (m, 1 H), 4.43 (d, $J = 5.3$, 1 H), 4.09 (t, $J = 6.9$, 2 H), 4.03 (d, $J = 13.0$, 1 H), 3.67 (dd, $J = 10.3$, 13.3, 1 H), 3.51 (s, 9 H), 2.79 (dd, $J = 5.7$, 17.0, 1 H), 2.66 (dd, $J = 7.0$, 17.1, 1 H), 1.80–1.60 (m, 4 H), 1.26 (brd s, 20 H), 0.88 (t, $J = 6.6$, 3 H); LSIMS (NBA) m/e 358.1 for $\text{C}_{21}\text{H}_{44}\text{NO}_3$ (cation).

Lauryl carnitine ester (2d): yield 77%; $^1\text{H NMR}$ (CDCl_3) δ 4.80 (m, 1 H), 4.43 (d, $J = 5.3$, 1 H), 4.09 (t, $J = 6.5$, 2 H), 4.03 (d, $J = 10.9$, 1 H), 3.67 (dd, $J = 10.2$, 13.2, 1 H), 3.52 (s, 9 H), 2.79 (dd, $J = 5.7$, 17.1, 1 H), 2.67 (dd, $J = 7.0$, 17.1, 1 H), 1.63 (t, $J = 6.6$, 2 H), 1.26 (brd s, 18 H), 0.88 (t, $J = 6.6$, 3 H); LSIMS (NBA) m/e 330.3 for $\text{C}_{19}\text{H}_{40}\text{NO}_3$ (cation).

Oleyl Carnitine Ester (2e). *cis*-1-Iodooctadec-9-ene was prepared from oleyl alcohol with methyltriphenoxyposphonium iodide according to Verheyden and Moffatt³³ and used to prepare 2e: yield 85%; $^1\text{H NMR}$ (CDCl_3) δ 5.33–5.45 (m, 2 H), 4.77 (m, 1 H), 4.05–4.20 (m, 3 H), 3.55–3.7 (m, 2 H), 3.50 (s, 9 H), 2.84 (dd, $J = 6.3$, 17.1, 1 H), 2.66 (dd, $J = 8.2$, 17.1, 1 H), 1.9–2.1 (brd m, 4 H), 1.55–1.7 (m, 2 H), 1.2–1.45 (m, 22 H), 0.88 (t, $J = 6.6$, 3 H); LSIMS (NBA) m/e 412.4 for $\text{C}_{25}\text{H}_{50}\text{NO}_3$ (cation).

General Procedure for the Preparation of Alkyl Acyl Carnitine Esters. Example: Stearyl Stearoyl Carnitine Ester (Stearyl 3-Stearoyloxy-4-trimethylammonium Butyrate Chloride, 4a). To a solution of stearic acid (2.0 g, 7.04 mmol) in CHCl_3 (fresh dried, 30 mL) was added 1,1'-carbonyldiimidazole (0.736 g, 3.70 mmol), and the mixture was stirred at room temperature under argon for 5 h. The formed white precipitate (byproduct) was removed by filtration, and the filtrate was evaporated under reduced pressure to give the stearic anhydride as a white solid. IR showed an absorption at 1804.5 cm^{-1} . The anhydride was used for next step reaction without further purification. A solution of the stearic anhydride (1.94 g, 3.52 mmol), stearyl carnitine ester (0.953 g, 1.76 mmol), and 4-(dimethylamino)pyridine (0.429 g, 3.52 mmol) in CHCl_3 (dry, 15 mL) was stirred at room temperature under argon for 4 days. The solvent was removed under reduced pressure, and the residue was washed twice by cold diethyl ether. The solid was chromatographed on a silica gel column using $\text{MeOH}-\text{CHCl}_3$ (1:5) as eluant to give the SSCE iodide. The iodide was exchanged by chloride with an anion exchange column to give 0.872 g (69%) of stearyl stearyl carnitine ester chloride (4a) as a white solid: $^1\text{H NMR}$ (300 MHz, CDCl_3) δ 5.67 (q, 1 H), 4.32 (d, $J = 14.3$, 1 H), 4.07 (m, 3 H), 3.51 (s, 9 H), 2.82 (t, $J = 5.9$, 2 H), 2.33 (t, $J = 7.6$, 2 H), 1.59 (brd m, 4 H), 1.25 (broad s, 58 H), 0.88 (t, $J = 6.6$, 6 H); LSIMS (NBA) m/e 680.6 for M^+ ($\text{C}_{43}\text{H}_{86}\text{NO}_4$). Anal. ($\text{C}_{43}\text{H}_{86}\text{ClNO}_4 \cdot \text{H}_2\text{O}$) C, H, N.

By this procedure were prepared the following alkyl acyl carnitine esters.

L-Stearyl stearyl carnitine ester (L-stearyl 3-stearoyloxy-4-trimethylammonium butyrate chloride, 4a') was prepared with the same procedure using L-carnitine as starting material. Analytical data are the same as for 4a.

Stearyl oleoyl carnitine ester (stearyl 3-oleoyloxy-4-trimethylammonium butyrate chloride, 4b): yield 41%; $^1\text{H NMR}$ (300 MHz, CDCl_3) δ 5.67 (m, 1 H), 5.35 (m, 2 H), 4.33 (d, $J = 14.5$, 1 H), 4.08 (m, 3 H), 3.48 (s, 9 H), 2.83 (dd, $J = 4.4$, 6.8, 2 H), 2.34 (dd, $J = 6.3$, 7.7, 2 H), 2.02 (brd m, 4 H), 1.26 (brd m, 54 H), 0.88 (t, $J = 6.7$, 6 H); LSIMS (NBA) m/e 678.7 for M^+ ($\text{C}_{43}\text{H}_{84}\text{NO}_4$). Anal. ($\text{C}_{43}\text{H}_{84}\text{ClNO}_4 \cdot \text{H}_2\text{O}$) C, H, N.

Palmityl palmitoyl carnitine ester (palmityl 3-palmitoyloxy-4-trimethylammonium butyrate chloride, 4c): yield 65%; $^1\text{H NMR}$ (300 MHz, CDCl_3) δ 5.67 (q, 1 H), 4.33 (d, $J = 14.0$, 1 H), 4.07 (m, 3 H), 3.51 (s, 9 H), 2.82 (t, $J = 5.9$, 2 H), 2.33 (t, $J = 7.6$, 2 H), 1.59 (brd m, 4 H), 1.25 (brd s, 58 H), 0.88 (t, $J = 6.52$, 6 H); LSIMS (NBA) m/e 680.6 for M^+ ($\text{C}_{39}\text{H}_{78}\text{NO}_4$). Anal. ($\text{C}_{39}\text{H}_{78}\text{ClNO}_4 \cdot \text{H}_2\text{O}$) C, H, N.

Myristyl myristoyl carnitine ester (myristyl 3-myristoyloxy-4-trimethylammonium butyrate chloride, 4d): yield 35%; $^1\text{H NMR}$ (300 MHz, CDCl_3) δ 5.67 (q, 1 H), 4.32 (d, $J = 13.8$, 1 H), 4.07 (m, 3 H), 3.50 (s, 9 H), 2.82 (t, $J = 6.1$, 2 H), 2.33 (t, $J = 7.6$, 2 H), 1.61 (brd m, 4 H), 1.26 (brd s, 42 H), 0.88 (t, 6 H); LSIMS (NBA) m/e 568.6.7 for M^+ ($\text{C}_{35}\text{H}_{70}\text{NO}_4$). Anal. ($\text{C}_{35}\text{H}_{70}\text{ClNO}_4 \cdot 1/2\text{H}_2\text{O}$) C, H, N.

L-Myristyl myristoyl carnitine ester (myristyl 3-myristoyloxy-4-trimethylammonium butyrate chloride, 4d') was prepared with the same procedure using L-carnitine as starting material. Analytical data are the same as for 4d, mp 157 °C dec.

Lauryl lauroyl carnitine ester (lauryl 3-lauroyloxy-4-trimethylammonium butyrate chloride, 4e): yield 37%; $^1\text{H NMR}$ (300 MHz, CDCl_3) δ 5.64 (m, 1 H), 4.28 (d, $J = 14.0$, 1 H), 4.07 (m, 3 H), 3.50 (s, 9 H), 2.82 (m, 2 H), 2.33 (t, $J = 7.6$, 2 H), 1.61 (brd m, 4 H), 1.26 (brd s, 38 H), 0.88 (t, 6 H); LSIMS (NBA) m/e 512.46 for M^+ ($\text{C}_{31}\text{H}_{62}\text{NO}_4$). Anal. ($\text{C}_{31}\text{H}_{62}\text{ClNO}_4 \cdot 2 1/2\text{H}_2\text{O}$) C, H, N.

Oleyl oleoyl carnitine ester (oleyl 3-oleoyloxy-4-trimethylammonium butyrate chloride, 4f): yield 28%; $^1\text{H NMR}$ (300 MHz, CDCl_3) δ 5.66 (m, 1 H), 5.35 (m, 4 H), 4.32 (d, $J = 14.6$, 1 H), 4.09 (m, 3 H), 3.48 (s, 9 H), 2.82 (m, 2 H), 2.33 (t, $J = 7.6$, 2 H), 2.00 (brd m, 8 H), 1.1–1.4 (brd m, 46 H), 0.88 (t, $J = 6.7$, 6 H); LSIMS (NBA) m/e 676.6 for M^+ ($\text{C}_{43}\text{H}_{82}\text{NO}_4$). Anal. ($\text{C}_{43}\text{H}_{82}\text{ClNO}_4 \cdot 2\text{H}_2\text{O}$) C, H, N.

Differential Scanning Calorimetry (DSC). The chloroform solutions of the lipids were placed in glass vials, and the solvent was removed with a rotary evaporator under reduced pressure. The residues were further dried in high vacuum overnight to give thin films of the lipids in the tubes. Sterile water was added, and the tubes were sealed under argon, warmed to 5 °C above the transition temperature, and then vortexed for 1 min. The heating and vortexing process was repeated three times, and the samples were degassed for 1 h, resulting in multilamellar vesicles (2.5 mM) which were used for DSC measurements. Thermograms were measured on a Microcal scanning calorimeter (MC-2, MicroCal, Inc.); samples were scanned at rate of 1 °C/min.

Monolayer Studies. Lipid monolayers were formed by adding a chloroform solution of the lipid dropwise onto the aqueous phase in a Langmuir–Wilhelmy surface balance trough. The trough was 440 cm long, 10 cm wide with a maximum surface area of 396.9 cm² and aqueous subphase capacity of 200–500 mL. The aqueous subphase buffer was the same as used in transfection procedure: 150 mM NaCl, 20 mM HEPES, pH 7.4, unless indicated elsewhere. After the spreading and forming of the lipid monolayer (15 min), the surface area was compressed using a moving bar driven by a digital controlled step motor. The initial surface area was 396.9 cm², the final area was 36.5 cm², and the compression velocity was about 16 cm²/min. During the whole compressing process, surface pressure π and surface potential V of the monolayer film were monitored using a Wilhelmy plate and an ionizing electrode, respectively.³² All data were collected at 1 s intervals and processed with Labview program on a Macintosh computer. The surface pressure–molecular area isotherm (π - A curve) and the surface potential–molecular area isotherm (V - A curve) are then displayed to form these data.

Preparation of Liposomes. A chloroform solution of the alkyl acyl carnitine ester alone or in combination with other helper lipids was placed in a rotary evaporator and the solvent removed under vacuum. The resulting thin film of lipid was dried overnight under a high vacuum. For β -galactosidase transfection studies in cell culture, the lipidic thin film was hydrated by sterile water into a 5 mM suspension followed by vortexing for 1 min. The hydrated lipids were sonicated for 20 min under argon at a temperature 5 °C above T_m to form a transparent liposome suspension. The liposome suspension was stored at 4 °C under argon and resonicated for 5 min before using. For luciferase transfection studies in mice, the lipidic thin film was hydrated by 10% HEPES (pH 7.4) into a 10 mM suspension followed by vortexing for 1 min. The hydrated lipids were warmed to 5 °C above T_m and then extruded through 200 nm filter to form an liposome suspension.

Particle Diameter and ζ Potential Measurements. To measure the particle diameter and ζ potential, the liposome suspension was diluted in sterile water to 0.5 μ M. The DNA–liposome complexes used for size and ζ potential measurements were taken from the same suspension used in cell culture transfection studies. The particle size of liposomes and DNA–liposome complexes were measured using dynamic light scattering on a sub-micron particle analyser (Coulter N4, Coulter Electronic, Inc.). The ζ potential of the liposomes were determined at identical lipid and buffer concentrations using a laser electrophoretic mobility instrument, ζ sizer (model 4, Malvern Instruments Ltd.).

CV-1 Cell Transfection Protocol. Formation of cationic lipid–DNA complexes was done in a 96-well plate similar to the method described by Felgner and co-workers.⁹ CV-1 cells (monkey fibroblast) were seeded onto a 96-well microtiter plate at 2 000 cells/well in DME-H21 media containing 10% FCS and antibiotics (100 units/mL penicillin) and grown overnight at 37 °C in a humidified atmosphere containing 5% CO₂. A solution of β -galactosidase plasmid DNA in sterile water (75 μ L, 24 ng/ μ L) was added into a 96-well microtiter plate containing 75 μ L/well of the indicated amount of alkyl acyl carnitine esters in sterile water to give the DNA–liposome

complexes. The complexes were left at room temperature for 20–30 min before use in transfection. The cells in 100 μ L of serum-free DME-H21 media were transfected by addition of 50 μ L of the liposome–DNA complexes per well. The cells were incubated at 37 °C for 5 h, and the complex-containing media was replaced by 150 μ L per well of DME-H21 containing 10% FCS. The cells were cultured for additional 48 h at 37 °C. Then, the cells were washed with 100 μ L of HBS per well and lysed by 50 μ L of Triton XT-100 (0.3%) in Tris buffer (pH 8, 0.25 mM). After completion of cell lysis, 50 μ L per well of HBS containing 0.1% of FCS was added followed by addition of 150 μ L of *O*-nitrophenyl- β -D-galactopyranoside (2 μ g/ μ L). β -Galactosidase gene expression was quantitated by measuring the optical density at λ_{630} with an automatic ELISA plate reader (MR 700, Dynatech Laboratories Inc.) and comparing the resulting absorbance to that resulting from a standard curve of bacterial β -galactosidase (Sigma).

Female ICR Mice Transfection Protocol. Formation of cationic lipid–DNA complexes were similar to the method described by Barron and co-workers.³⁴ Female ICR mice were bred for 3–6 weeks until they reached weight of about 30 g. On the day of the experiment the mice were fasted for 6 h prior to administration of the complexes. Into each mouse was injected *iv* at caudal vein 100 μ L of cationic lipid–DNA complex containing 30 μ g of RSV-Luc plasmid DNA. Food was provided 0.5 h after injection, and the animals were sacrificed after 48 h. The heart, lung, and about 300 mg of liver of each mouse was excised and transferred into separate tubes with 1.2 mL of lysis buffer (Promega) and 1 g of zirconium beads. The tissues were then homogenized in a Mini-Beadbeater (Biospec Products, Inc., Bartlesville, OK), two times for 10 s. The homogenate was clarified by centrifugation in a microcentrifuge at 12 000 rpm for 7 min. The supernatant was transferred into separate tubes, and 10 μ L of the supernatant was used to measure luciferase according to the recommendations of the manufacturer (Promega; Luciferase Assay System, no. E1501) using a Optocomp I luminometer (MGM Inc.; Hamden, CT). Protein concentration of the cell lysates was determined using the Bio-Rad protein assay (Richmond, CA) in a 96-well plate format according to the manufacturer's specifications.

Toxicity Assay. The effect of the alkyl acyl carnitine esters on cell growth was assessed by measuring total protein content after transfection as well as by using a colorimetric dye reduction assay.³² CV-1 cells were plated at a density of about 2×10^4 cells per well in 100 μ L of DMF H-21 containing 10% FCS in 96-well trays, and the transfection protocol was performed as described above in 150 μ L of media. After an incubation at 37 °C in 5% CO₂ for 48 h, 10 μ L per well of 3-(4,5-dimethylthiazol-2-yl)-2,5-diphenyltetrazolium bromide (MTT, 5 mg/mL) was added, and the mixture was allowed to react for 4 h at 37 °C. Solubilizing solution (50% of DMF–20% of SDS at pH 4.7, 200 μ L) was added and the plate incubated for 30 min at room temperature. Absorbance at 570 nm was measured using an automatic ELISA plate reader (MR 700, Dynatech Laboratories Inc.). Results are expressed as percent reduction in cell viability = $\{1 - [\text{OD}_{570}(\text{treated cells}) - \text{background}] / [\text{OD}_{570}(\text{untreated cells}) - \text{background}]\} \times 100$.

Acknowledgment. We are grateful to Dr. Carl Redemann, Dr. Tara Buckley Wyman, Dr. Mary Tang, and Gary Green for helpful discussions and technical assistance. Thanks are also extended to the UCSF mass spectrometry facility supported by the NIH Division of Research Resources, Grant RRO1614, and to Dr. Jon Goerke for kindly allowing us to use his monolayer surface tension instrument as well as his advice and comments on the measurements. Dr. Szoka has a financial interest in and serves as a consultant to GeneMedicine, Inc., a biotechnology company developing gene medicines. This work was supported by the National Institute of Health Grant P30 DK47766, DK46052 and The California TRDRP 6RT-0109.

References

- (1) Abbreviations used: Chol, cholesterol; DDAB, dimethyldioctadecylammonium bromide; DOPC, dioleoylphosphatidylcholine; DOPE, dioleoylphosphatidylethanolamine; DOTAP, *N*-[1-(2,3-dioleoyloxy)propyl]-*N,N,N*-trimethylammonium chloride; LLCE, lauryl 3-lauroyloxy-4-trimethylammonium butyrate chloride; MOG, monooleoylglycerol; MMCE, myristyl 3-myristoyloxy-4-trimethylammonium butyrate chloride; OOCE, oleyl 3-oleoyloxy-4-trimethylammonium butyrate chloride; PPCE, palmityl 3-palmitoyloxy-4-trimethylammonium butyrate chloride; SOCE, stearyl 3-oleoyloxy-4-trimethylammonium butyrate chloride; SSCE, stearyl 3-stearoyloxy-4-trimethylammonium butyrate chloride; T_m , phase transition temperature.
- (2) Wolff, J. A. Gene therapy—a primer. *Pediatr. Ann.* **1993**, *22*, 312–321.
- (3) (a) Felgner, P. L. Particulate systems and polymers for *in vitro* and *in vivo* delivery of polynucleotides. *Adv. Drug Delivery Rev.* **1990**, *5*, 163–187. (b) Behr, J. P. Gene transfer with synthetic cationic amphiphiles: prospects for gene therapy. *Bioconjug. Chem.* **1994**, *5*, 382–389.
- (4) Felgner, P. L.; Gadek, T. R.; Holm, M.; Roman, R.; Chan, H. W.; Wenz, M.; Northrop, J. P.; Ringold, G. M.; Danielsen, M. Lipofection: a highly efficient, lipid-mediated DNA-transfection procedure. *Proc. Natl. Acad. Sci. U.S.A.* **1987**, *84*, 7413–7417.
- (5) Behr, J. P.; Demeneix, B.; Loeffler, J. P.; Perez-Mutul, J. Efficient gene transfer into mammalian primary endocrine cells with lipopolyamine-coated DNA. *Proc. Natl. Acad. Sci. U.S.A.* **1989**, *86*, 6982–6986.
- (6) Leventis, R.; Silviu, J. R. Interactions of mammalian cells with lipid dispersions containing novel metabolizable cationic amphiphiles. *Biochim. Biophys. Acta* **1990**, *1023*, 124–132.
- (7) Gao, X.; Huang, L. A novel cationic liposome reagent for efficient transfection of mammalian cells. *Biochem. Biophys. Res. Commun.* **1991**, *179*, 280–285.
- (8) Legendre, J. Y.; Szoka, F., Jr. Delivery of plasmid DNA into mammalian cell lines using pH-sensitive liposomes: comparison with cationic liposomes. *Pharm. Res.* **1992**, *9*, 1235–1242.
- (9) Felgner, J. H.; Kumar, R.; Sridhar, C. N.; Wheeler, C. J.; Tsai, Y. J.; Border, R.; Ramsey, P.; Martin, M.; Felgner, P. L. Enhanced gene delivery and mechanism studies with a novel series of cationic lipid formulations. *J. Biol. Chem.* **1994**, *269*, 2550–2561.
- (10) Jaaskelainen, I.; Monkkonen, J.; Urtti, A. Oligonucleotide-cationic liposome interactions. A physicochemical study. *Biochim. Biophys. Acta* **1994**, *1195*, 115–123.
- (11) Bremer, J. Carnitine-metabolism and functions. *Physiol. Rev.* **1983**, *63*, 1420–1480.
- (12) Bach, A. C. Carnitine in human nutrition. *Z. Ernährungswiss.* **1982**, *21*, 257–265.
- (13) Siliprandi, N.; Di Lisa, F.; Pivetta, A.; Miotto, G.; Siliprandi, D. Transport and function of L-carnitine and L-propionylcarnitine: relevance to some cardiomyopathies and cardiac ischemia. *Z. Kardiol.* **1987**, *5*, 34–40.
- (14) Pourfarzam, M.; Bartlett, K. Synthesis, characterization and high-performance liquid chromatography of C6-C16 dicarboxylmono-coenzyme A and -mono-carnitine esters. *J. Chromatogr.* **1991**, *570*, 253–276.
- (15) Reed, K. W.; Ueda, C. T.; Murray, W. J.; Augustine, S. C. Radiolabeled 9- or 10- monoiodostearic acid and 9- or 10- monoiodostearyl carnitine-I. Synthesis and purification. *Int. J. Rad. Appl. Instrum. [a]* **1989**, *40*, 27–31.
- (16) Cervenka, J.; Osmundsen, H. Synthesis of unsaturated carnitine esters with *N*-acyl imidazoles. *J. Lipid. Res.* **1982**, *23*, 1243–1246.
- (17) Holland, P. C.; Sherratt, H. S. 4-Pentenylcarnitine, cyclopropanecarbonylcarnitine, and cyclobutanecarbonylcarnitine. *Methods Enzymol.* **1981**, *72*, 616–619.
- (18) Squire, R. S. Synthesis and purification of radioactive fatty acylcarnitines of high specific activity. *Anal. Biochem.* **1991**, *197*, 104–107.
- (19) Criddle, D. N.; Dewar, G. H.; Radniknam, M.; Wathey, W. B.; Woodward, B. The synthesis, and structure-activity relationships of some long chain acyl carnitine esters on the coronary circulation of the rat isolated heart. *J. Pharm. Pharmacol.* **1991**, *43*, 636–639.
- (20) Yamamoto, H.; Okuyama, M.; Yamaguchi, S. Pitfalls in the assay of acylcarnitine. *Clin. Chem.* **1986**, *32*, 393–394.
- (21) Cederblad, G.; Harper, P. More on determination of acylcarnitine [letter]. *Clin. Chem.* **1986**, *32*, 2117–2118.
- (22) Jones, M. N.; Chapman, D. *Micelles, Monolayers, and Biomembranes*; Wiley-Liss, Inc.: New York, 1995.
- (23) Surface potential (ΔV) of a lipid monolayer is believed to consist of two parts:

$$\Delta V = \varphi(0) + \frac{12.0\pi}{A} \sum_i \mu_{iL}$$

- where $\varphi(0)$ describes the electrostatic potential of the monolayer due to the surface charge density of the film, and the remaining part is a conventional expression of the surface potential due to the vertical components of the dipole moments of the lipids μ_{iL} .
- (24) Sautereau, A. M.; Betermier, M.; Altibelli, A.; Tocanne, J. F. Adsorption of the cationic antitumor drug celiptium to phosphatidylglycerol in membrane model systems. Effect on membrane electrical properties. *Biochim. Biophys. Acta* **1989**, *978*, 276–282.
 - (25) Shimooka, T.; Shibata, A.; Terada, H. The local anesthetic tetracaine destabilizes membrane structure by interaction with polar headgroups of phospholipids. *Biochim. Biophys. Acta* **1992**, *1104*, 261–268.
 - (26) Gershon, H.; Ghirlando, R.; Guttman, S. B.; Minsky, A. Mode of formation and structural features of DNA-cationic liposome complexes used for transfection. *Biochemistry* **1993**, *32*, 7143–7151.
 - (27) Smyth-Templeton, N.; Lasic, D. D.; Frederik, P. M.; Strey, H. H.; Roberts, D. D. and Pavlakis, G. N. Improved DNA:liposome complexes for increased systemic delivery and gene expression. *Nature Biotechnol.* **1997**, *15*, 647–652.
 - (28) Akao, T.; Osaki, T.; Ito, A.; Kunitake, T. Correlation between physicochemical characteristics of synthetic cationic amphiphiles and their DNA transfection ability. *Bull. Chem. Soc. Jpn.* **1991**, *64*, 3677–3681.
 - (29) Wrobel, I.; Collins, D. Fusion of cationic liposomes with mammalian cell occurs after endocytosis. *Biochim. Biophys. Acta* **1995**, *1235*, 296–304.
 - (30) Xu, Y.; Szoka, F. C., Jr. Mechanism of DNA release from cationic liposome/DNA complexes used in cell transfection. *Biochemistry* **1996**, *35*, 5616–5623.
 - (31) Mosmann, T. Rapid colorimetric assay for cellular growth and survival: application to proliferation and cytotoxicity assays. *J. Immunol. Methods* **1983**, *65*, 55–63.
 - (32) Gaines, G. L. *Insoluble Monolayers at Liquid-gas Interfaces*; Interscience Publishers: New York, 1966.
 - (33) Verheyden, J. P. H.; Moffatt, J. G. Halo sugar nucleosides. I. Iodination of the primary hydroxyl groups of nucleosides with methyltriphenoxyphosphonium iodide. *J. Org. Chem.* **1970**, *35*, 2319–2326.
 - (34) Barron, L. G.; Meyer, K. B.; Szoka, F. C., Jr. Effects of complement depletion on the pharmacokinetics and gene delivery mediated by cationic lipid-DNA complexes. *Hum. Gen. Ther.* **1998**, *9*, 315–323.

JM950802I